JOURNAL OF CATALYSIS 58, 82–94 (1979)

Active States of Rhodium in Rhodium Exchanged Y Zeolite Catalysts for Hydrogenation of Ethylene and Acetylene and Dimerization of Ethylene Studied with X-Ray Photoelectron Spectroscopy

YASUAKI OKAMOTO, NOBUMASA ISHIDA, TOSHINOBU IMANAKA, AND SHIICHIRO TERANISHI

Department of Chemical Engineering, Faculty of Engineering Science, Osaka University, Toyonaka, Osaka 560, Japan

Received September 8, 1978

Rh-Y zeolite catalysts were investigated with X-ray photoelectron spectroscopy (XPS) techniques. It was found, for the first time, that Rh(I) was formed in Rh-Y zeolites as a significantly stable intermediate during the reduction of Rh(III) to Rh metal by heat treatment in vacuum. It was revealed that Rh(I) in Rh-Y zeolites was active for the hydrogenation and the dimerization of ethylene, whereas Rh metal was active for the hydrogenation of both ethylene and acetylene. Strong correlations were established between homogeneous Rh complex catalysts and Rh-Y catalysts both in the active oxidation states of Rh and the effect of additives on the reactions. Furthermore, XPS was successfully applied to define not only the chemical nature but also the structure of Rh in zeolites. The structure of Rh in Rh-Y zeolite was suggested to correlate strongly with the chemical nature of Rh.

INTRODUCTION

It is very interesting to establish relationships regarding the active states of transition metal cations for catalytic reactions between homogeneous transition metal complex catalysts and transition metal-exchanged zeolite catalysts, in order to develop zeolite catalysts and to understand well reactions on zeolites. For the sake of establishing such relationships, it is necessary to characterize the chemical states of transition metal cations in zeolites. The XPS (X-ray photoelectron spectroscopy or ESCA) technique is one of the most adequate techniques for this purpose, since it usually provides information on all the chemical states of transition metal cations regardless of paramagnetic or diamagnetic species and since it is quantitative enough to compare with catalytic properties.

It is well known that transition metals in zeolites show catalytic activities in their cationic forms for a variety of reactions such as oxidations (*1–3*), the cyclotrimerization of acetylene (*4*), and the amination of chlorobenzene (*5*) and in their finely dispersed metallic forms for hydrogenation (*6*), hydrocracking (*7*), hydroisomerization (*8*), and polymerization (*9*). These facts suggest that there are some analogies between transition metal complex catalysts and transition metal cations in zeolites. In this study, Rh-exchanged Y zeolites were investigated to establish further relationships between them.

XPS studies of transition metal cation-exchanged zeolite catalysts have been shown to be very powerful aids to understanding the behavior of the cations under reductive or oxidative conditions. Minachev

0021-9517/79/070082-13$02.00/0

and his co-workers (*10*) studied Cu-, Ni-, Co-, Fe-, Zn-, Ag-, Pd-, and Pt-Y zeolites with XPS and reported the formations of intermediate oxidation states of Ni and Cu [Ni(I) and Cu(I)] by reduction with CO. Using XPS, Vedrine *et al.* (*11*) found Pd(I) formation in Pd-Y zeolite reduced with H_2 at room temperature, which is in agreement with ESR results (*12*). It has been noted with ESR that Ni(I) is formed in Ni-Y zeolite during the cyclotrimerization of acetylene (*4*). Very recently, Kasai *et al.* (*13*) confirmed the formation of Ni(I) and Cu(I) in Ni- and Cu-Y zeolites exposed to NO and CO, using ESR and ir techniques. It will be instructive to study the catalytic properties of such intermediate oxidation states of a cation in zeolite in connection with transition metal complex catalysts. However, no such investigations have been reported up to now. In this paper, Rh-Y zeolite catalysts are studied with XPS in order to characterize well the oxidation states of Rh in the zeolite catalysts and to correlate them with the catalytic activities of the Rh-Y zeolites. No XPS study of Rh-Y zeolite has been published so far.

It is well known that Rh complexes, such as $RhCl(PPh_3)_3$, are excellent catalysts for the hydrogenation (*14*) and the dimerization (*15*) of olefins. The mechanisms of these reactions have been extensively studied and are well understood. In the case of Rh-Y catalysts, the dimerization of ethylene was reported by Yashima *et al.* (*9*). They have concluded that atomically dispersed Rh metal is an active species in the reaction. However, it seems that no decisive evidence was presented. Their conclusions appear somewhat unusual, compared with the results on homogeneous Rh complex catalysts (*15*).

The main objective of this study was to find similarities and discrepancies in the catalytic properties of Rh in homogeneous Rh complexes and heterogeneous Rh-Y zeolite catalysts. The hydrogenation of ethylene and acetylene and the dimerization of ethylene on Rh-Y zeolite catalysts were studied, coupled with the XPS studies of the Rh-Y catalysts.

EXPERIMENTAL METHODS

Catalysts. Rh-Y zeolite catalysts were prepared by a conventional cation exchange procedure using Linde SK-40 Y-type zeolite (Si/Al = 2.4) and a 0.013 *N* aqueous solution of $RhCl_3 \cdot 3H_2O$ at 90°C. After vigorous stirring for several hours, the color from the filtrate disappeared completely. Then the exchanged zeolite catalysts were filtered and washed thoroughly with deionized water, followed by drying at 80°C for 16 hr. The degrees of ion exchange were calculated assuming that all the Rh ions used were exchanged. In this study, 18 and 50% exchanged Rh-Y zeolite catalysts were prepared. These catalysts are denoted Rh-Y (18%) and Rh-Y (50%) hereafter.

Apparatus and procedure. The hydrogenation of ethylene and acetylene and the dimerization of ethylene were carried out over the Rh-Y catalysts using a static reactor (volume, ca. 80 ml, without circulation) maintained at 20°C in a water bath. In all experiments, 0.1 g of the Rh-Y catalyst was used after activations at various temperatures in a vacuum (ca. 1×10^{-3} Torr; 1 Torr = 133.3 N/m^2) for 30 min. Diffusion effects and temperature changes of the catalysts expected in cases of hydrogenation due to exothermic reactions were neglected, since the primary focus of our study was the relative activities of the catalysts. However, a knowledge of the exact activities of the catalysts for the reactions will not alter the results regarding the relative activities of the catalysts under investigation.

In the cases of hydrogenation, H_2/ethylene and H_2/acetylene ratios were 1.05 and 1.06, respectively. The initial total pressure of the reactant was 76 or 100 Torr.

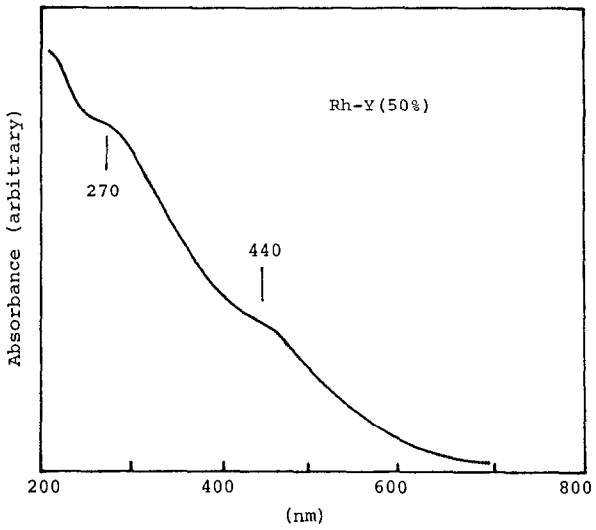

FIG. 1. Diffuse reflectance spectrum of the Rh-Y (50%) catalyst before activation.

The conversions of ethylene and acetylene were calculated after 2 or 5 min of reaction at 20°C. The reaction mixtures were analyzed with a mass spectrometer (Hitachi RMS-4), taking into account the pattern coefficients and sensitivity factors of ethylene, acetylene, and ethane, where the sensitivity factors were determined using Ar (m/e = 40) as a standard.

The catalytic activities of the Rh-Y catalysts for the dimerization of ethylene were measured by the pressure drop of the system. The initial pressure of ethylene was 80 Torr, and the reaction temperature was maintained at 20°C. The rates of pressure drop at a reaction time of 10 min were employed as the activities of the Rh-Y catalysts to avoid the effects of the initial fast adsorption of ethylene on the catalysts. The reaction mixtures were analyzed with a gas chromatograph.

XPS spectra were measured on a Hitachi 507 photoelectron spectrometer equipped with a cylindrical mirror analyzer using AlK$\alpha_{1,2}$ radiation. The catalysts and Rh compounds were pressed by hand on a grid attached to a sample holder made of stainless steel. The binding energies for the Rh compounds were referenced to the contaminant or phenyl carbon (C 1*s* = 285.0 eV), while the binding energies for the zeolite catalysts were corrected using the Al 2*s* level in the zeolites as an internal standard (Al 2*s* = 119.0 eV), since heat treatments may cause unavoidable shifts in the C 1*s* level and since the Al 2*s* binding energy values for the catalysts were 119.0 eV prior to heat treatments in a vacuum. All binding energies were measured with a precision of ±0.2 eV. The deconvolutions of the Rh 3*d* level for the Rh-Y catalysts were carried out using a Du Pont 310 curve resolver. The respective fractions of Rh(III), Rh(I), and Rh metal in the Rh were reproduced within an accuracy of ca. 3%.

ESR measurements of the catalyst samples were carried out at room temperature using a Japan Electronics Corp. ME-2X spectrometer.

Diffuse reflectance spectra of the Rh-Y zeolites were recorded in the range 200 to 800 nm by use of Hitachi 200-20 spectrophotometer against standards of alumina.

RESULTS

Reflectance spectra of the Rh-Y catalysts. The diffuse reflectance spectrum of the

Rh-Y (50%) catalyst is shown in Fig. 1. The Rh-Y (18%) showed a similar spectrum. Taking into account the facts that the Rh ion is trivalent and that the Cl/Rh atomic ratio is about 0.5, as shown later in this paper, it appears from Fig. 1 that Rh ion is exchanged as $Rh(H_2O)_x^{3+}$, $RhCl(H_2O)_x^{2+}$ (*16*), and probably hydroxo complexes.

Hydrogenation of ethylene on the Rh-Y catalysts. Shown in Fig. 2 are the conversions of ethylene to ethane for the Rh-Y (18%) and Rh-Y (50%) catalysts as a function of the activation temperature. In the case of the Rh-Y (18%), two activity maxima were observed around 200 and 400°C. The Rh-Y (50%) catalyst also showed two activity maxima around 250 and 500°C. These findings suggest that two kinds of active states of Rh are formed in the Rh-Y catalysts during the activation process.

Hydrogenation of acetylene on the Rh-Y (18%) catalysts. As shown in Fig. 3, only a single activity peak was observed around 400°C. This activation temperature is in good agreement with the temperature of the higher temperature (HT) peak in the hydrogenation of ethylene on the Rh-Y (18%) catalyst. This fact indicates that the active state of Rh corresponding to the activity peak at 400°C in Fig. 2 shows hydrogenation activities both for ethylene and acetylene, whereas the state of Rh corresponding to the lower temperature (LT) peak observed at 200°C is active merely for the hydrogenation of ethylene.

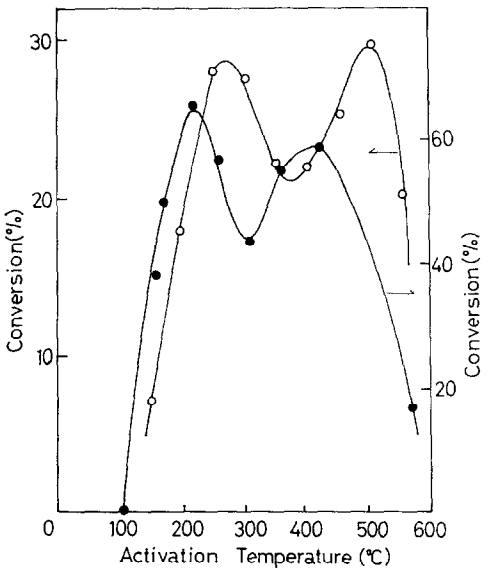

FIG. 2. Effect of activation temperature on the hydrogenation of ethylene over the Rh-Y (50%) and Rh-Y (18%) catalysts. ○, Rh-Y (50%): reaction time, 2 min; initial pressure, 100 Torr. ●, Rh-Y (18%): reaction time, 5 min; initial pressure, 76 Torr.

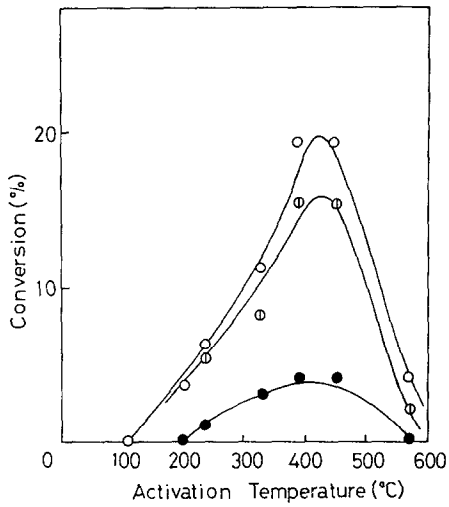

FIG. 3. Effect of activation temperature on the hydrogenation of acetylene over the Rh-Y (18%) catalyst. Reaction conditions: reaction time, 5 min; initial pressure, 76 Torr. ○, total conversion of acetylene; ⊕, conversion to ethylene; ●, conversion to ethane.

Dimerization of ethylene on the Rh-Y catalysts. The activities of the Rh-Y (50%) catalysts obtained from the pressure drop of ethylene are plotted in Fig. 4 as a function of the temperature of activation in vacuum. Only a single peak was observed around 250°C, in excellent agreement with the activation temperature corresponding to the LT activity maximum in the hydrogenation of ethylene (Fig. 2). Ethylene was selectively dimerized to *n*-butenes, as reported by Yashima *et al.* (*9*). The isomer distribution of the butenes was: 1-butene,

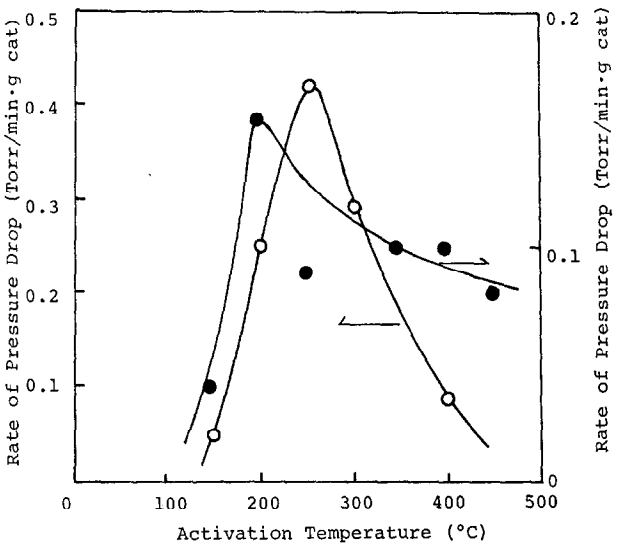

FIG. 4. Effect of activation temperature on the dimerization of ethylene over the Rh-Y (50%) (○) and Rh-Y (18%) (●) catalysts.

2%; *trans*-2-butene, 77%; and *cis*-2-butene, 21%, after the 2-hr reaction over the Rh-Y (50%) zeolite activated at 250°C, indicating almost an equilibrium isomer distribution. The isomerization of 1-butene was confirmed to proceed readily on the Rh-Y catalysts under similar conditions using ir techniques, in agreement with the results reported by Yashima and his coworkers (*9*). NH_4-Y zeolite (90% exchanged) activated at 400°C for 1 hr did not show a pressure drop except for a rapid initial pressure drop due to the adsorption of ethylene, and neither butene nor polymer was produced at 20°C. With the Rh-Y (18%) catalyst, a single activity peak was observed similar to the Rh-Y (50%) catalyst as shown in Fig. 4.

In order to estimate the active site for the dimerization of ethylene over the Rh-Y catalysts, the Rh-Y (50%) catalyst activated at 250°C was treated with pyridine, CO, H_2, HCl, and H_2O prior to the reaction. As shown in Fig. 5, the dimerization activity was depressed by the pretreatment with CO or pyridine. Carbon monoxide deactivated the catalyst much more than pyridine, in agreement with the results reported by Yashima *et al.* (*9*). Therefore, Rh is considered to be the active site for the reaction. This is consistent with the fact that H-Y zeolite shows no activity for the dimerization of ethylene. The effect of the pretreatments of the Rh-Y (50%) catalyst with H_2O, HCl, and H_2 on the dimerization activity are shown in Fig. 6. Water deactivated the catalyst very effectively, whereas hydrogen and an appropriate amount of HCl were found to activate the catalyst for the reaction. However, the pretreatments with too much HCl depressed the activity. These effects will be discussed below in connection with the results obtained with XPS.

Consequently, it is suggested that two kinds of Rh are present in the Rh-Y zeolite catalysts; one is responsible for the hydrogenation and the dimerization of ethylene and another for the hydrogenation of both ethylene and acetylene.

XPS studies of the Rh-Y catalysts. The XPS binding energies for some Rh compounds are summarized in Table 1. The XPS spectra of these compounds are shown in Fig. 7. The admission of HCl to $RhCl(PPh_3)_3$ caused a new peak around

310 eV, indicating the oxidative addition of HCl to $RhCl(PPh_3)_3$ to form a Rh(III) complex. The oxidative addition of H_2 to $RhCl(PPh_3)_3$ was also confirmed to proceed in a solid phase using XPS. The high binding energies of Rh(I) complexes containing CO as a ligand are considered to result from the strong π accepting nature of CO.

The XPS data for the Rh-Y (50%) and Rh-Y (18%) catalysts are listed in Tables 2 and 3. The XPS spectra of the Rh 3*d* level for the Rh-Y (50%) catalysts activated at various temperatures are shown in Fig. 8. It was revealed using the curve resolver that these spectra were composed of three kinds of Rh, that is, Rh(III) (Rh $3d_{\frac{5}{2}}$; 310.2 eV), Rh metal (307.5 eV), and the Rh cation for which the Rh $3d_{\frac{5}{2}}$ binding energy was 308.3 eV. ESR measurements showed no peak except a broad signal (g = 2.560, ΔH = ca. 1500 G) due to Rh metal and a weak signal (g = 2.001) due to carbonaceous deposits. These findings rule out the presence of Rh(II) as a stable intermediate in the zeolite catalysts, in agreement with the facts that Rh(II) complexes can be obtained only as special cases (*17*, *18*). Therefore, the Rh cation with the binding energy of 308.3 eV can be assigned to Rh(I), based on the ESR results and the binding energy.

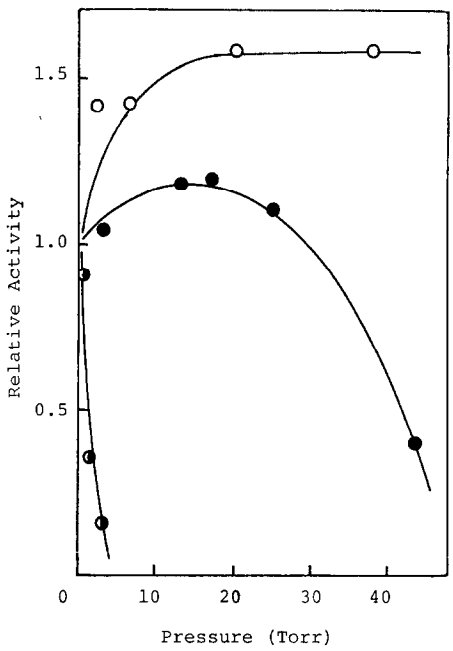

FIG. 6. Effect of pretreatments on the dimerization of ethylene over the Rh-Y (50%) catalyst activated at 250°C for 30 min. The catalyst was exposed to the indicated pressure of H_2 (○), HCl (●), and H_2O (◑) for 30 min, followed by evacuation for 30 min prior to the reaction. Pretreatment temperature: room temperature for H_2O and HCl; 50°C for H_2.

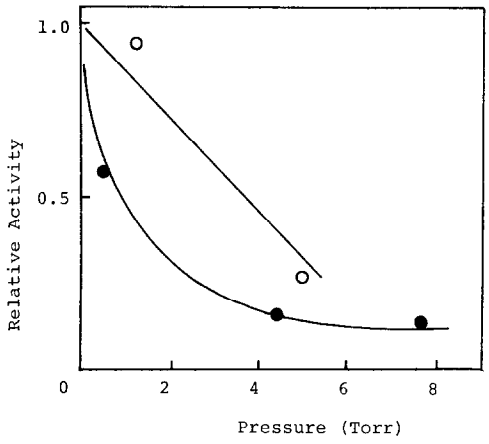

FIG. 5. Effect of pretreatments on the dimerization of ethylene over the Rh-Y (50%) catalyst activated at 250°C for 30 min. The catalyst was exposed to the indicated pressure of pyridine (○) and CO (●) at room temperature for 30 min, followed by evacuation at room temperature for 30 min prior to the reaction.

The respective fractions of Rh(III), Rh(I), and Rh metal in the Rh are shown

TABLE 1

Binding Energies (eV)[a] of Rh 3*d*, P 2*p*, and Cl 2*p* levels for Rh compounds

Sample	Rh $3d_{\frac{3}{2}}$	Rh $3d_{\frac{5}{2}}$	P 2*p*	Cl 2*p*
Rh metal	312.1	307.2		
$RhCl(PPh_3)_3$	312.5	307.8	131.7	198.2
$RhCl(CO)(PPh_3)_2$	313.6	309.0	131.7	198.7
$RhH(CO)(PPh_3)_2$	313.5	308.7	131.5	
$RhCl_3$	315.0	310.3		199.5
Rh_2O_3	313.3	308.4		

[a] C 1*s* = 285.0 eV

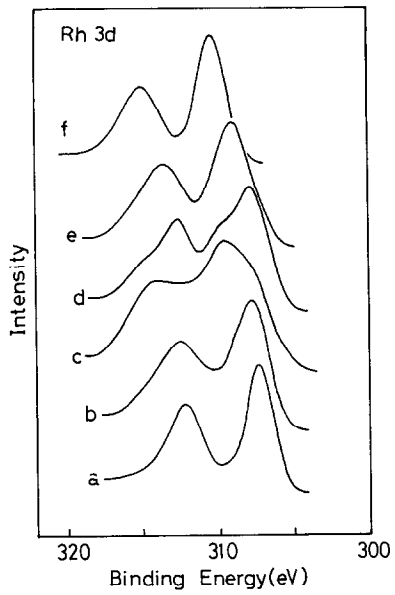

FIG. 7. XPS spectra of Rh 3*d* level for Rh compounds: (a) Rh metal, (b) $RhCl(PPh_3)_3$, (c) $RhCl(PPh_3)_3$ contacted with 80 Torr of HCl for 15 min at room temperature, (d) $RhCl(PPh_3)_3$ exposed to 30 Torr of H_2 for 16 hr at room temperature, (e) $RhCl(CO)(PPh_3)_2$, and (f) $RhCl_3$.

in Fig. 9 for the Rh-Y (50%) catalyst as a function of the activation temperature. The amount of Rh(I) increased with increasing activation temperatures and had

TABLE 2

Characterization of the Rh-Y (50%) Catalyst with XPS

Activation temperature (°C)	Binding energy (eV)[a]			Rh 3*d*/Al 2*s*	Cl/Rh[b]
	Rh $3d_{\frac{3}{2}}$	Rh $3d_{\frac{5}{2}}$	Si 2*s*		
—	315.1	310.2	153.4	61.9	0.59
150	313.8	309.1	153.4	64.4	0.55
200	313.0	308.3	153.3	66.4	0.50
250	312.7	308.2	153.5	65.9	0.41
300	312.6	308.2	153.4	39.6	0.26
350	312.4	307.8	153.4	26.0	0.02
450	311.6	307.5	153.3	28.4	0.04
500	312.3	307.6	153.4	32.1	0.01
550	312.2	307.5	153.4	23.1	0
650	311.8	307.2	153.3	27.4	0

[a] Al 2*s* = 119.0 eV.
[b] Atomic ratio.

TABLE 3

Characterization of the Rh-Y (18%) Catalyst with XPS

Activation temperature (°C)	Binding energy (eV)[a]		Rh 3*d*/Al 2*s*	Cl/Rh[b]
	Rh $3d_{\frac{3}{2}}$	Rh $3d_{\frac{5}{2}}$		
—	315.0	310.1	16.0	0.44
150	314.1	309.6	17.8	0.38
200	312.3	307.8	16.8	0.11
250	312.4	307.7	13.1	0.03
300	312.5	307.9	10.6	0
350	312.5	307.7	12.2	0
400	312.3	307.8	12.8	0
450	312.5	307.8	12.2	0

[a] Al 2*s* = 119.0 eV.
[b] Atomic ratio.

a maximum value around 250°C. Subsequently, it decreased with further increases in the treatment temperature. The fraction of Rh(III) decreased monotonically with

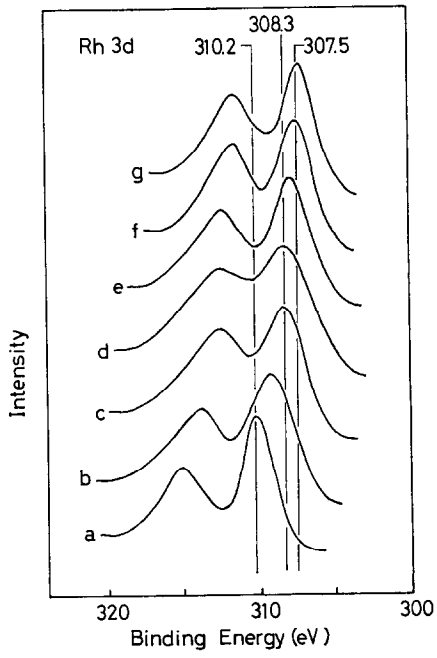

FIG. 8. XPS spectra of Rh 3*d* level for the Rh-Y (50%) catalyst activated at various temperatures: (a) before activation, (b) activated at 150°C, (c) at 250°C, (d) at 300°C, (e) at 350°C, (f) at 450°C, and (g) at 650°C for 30 min.

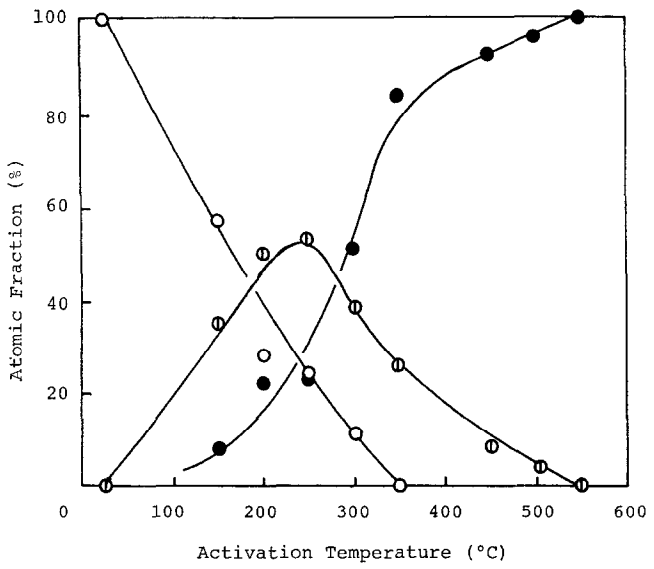

FIG. 9. Oxidation state of Rh in the Rh-Y (50%) catalyst as a function of activation temperature. ○, Rh(III) (Rh $3d_{\frac{5}{2}}$; 310.2 eV); ⊕, Rh(I) (308.3 eV); and ●, Rh metal (307.5 eV).

increasing activation temperatures and disappeared at 350°C, whereas the Rh metal fraction increased with increasing evacuation temperatures. In the case of the Rh-Y (18%) zeolite, composition changes similar to those shown in Fig. 9 were observed (Fig. 10). The Rh(I) concentration reached a maximum at 200°C. However, Rh(I) and Rh(III) were present even after a 450°C treatment. In Table 4, the ESR peak-to-peak intensities due to Rh metal are compared with the Rh metal fraction in the Rh-Y (18%) catalyst obtained from XPS. A good parallel relationship was observed, indicating the deconvolutions of Rh 3*d* levels in the Rh-Y catalysts to be reliable.

The XPS intensity ratio of Rh 3*d*/Al 2*s* and the atomic ratio of Cl/Rh are plotted against the activation temperature in Fig. 11 for the Rh-Y (50%) and in Fig. 12 for the Rh-Y (18%) zeolite catalysts. The Cl/Rh atomic ratios were calculated from the Cl 2*p*/Rh 3*d* XPS area intensity ratios of the catalysts calibrated using $RhCl_3$ and $RhCl(PPh_3)_3$ as standard compounds. The Cl/Rh atomic ratios decreased with increasing activation temperatures. Almost all chlorine was removed by activation in vacuum at 300 to 400°C. Nevertheless, the Rh 3*d*/Al 2*s* intensity ratios changed in complex manners for both Rh-Y catalysts. They increased slightly with low temperature treatments in vacuum [<200°C for the Rh-Y (18%) and <250°C for the Rh-Y (50%)] and decreased remarkably with higher temperature activation. Subsequently, small increases were observed, although they were not so apparent. Then, the Rh 3*d*/Al 2*s* ratios decreased again with further higher temperature treatments [>400°C for the Rh-Y (18%) and >500°C for the Rh-Y (50%)]. These observations indicate complex changes in the concentration and structure of Rh in the zeolite outermost surfaces during the activation process. The following important points are noted:

(1) The maxima in the Rh 3*d*/Al 2*s* ratios around 200 and 250°C for the Rh-Y (18%) and Rh-Y (50%) catalysts, respectively, correspond to the LT activity maxima observed in the hydrogenation of ethylene (Fig. 2) and to the single peaks

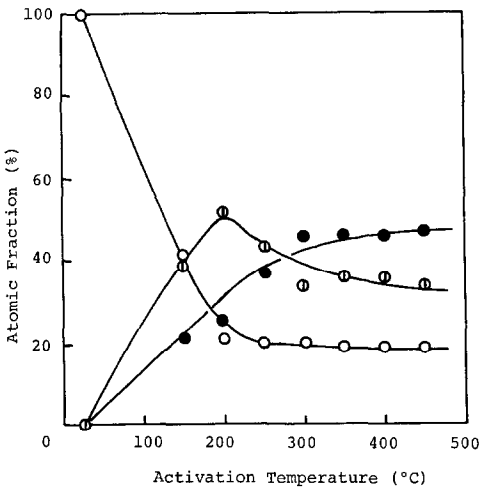

FIG. 10. Oxidation state of Rh in the Rh-Y (18%) catalyst as a function of activation temperature. ○, Rh(III) (Rh $3d_{\frac{5}{2}}$; 310.1 eV); ⓘ, Rh(I) (308.3 eV); and ●, Rh metal (307.5 eV).

observed in the dimerization of ethylene (Fig. 4) on both Rh-Y catalysts;

(2) the small higher temperature maxima in the Rh 3*d*/Al 2*s* ratios seem to correspond to the HT activity maxima in the hydrogenation of ethylene (Fig. 2) and to a maximum in the hydrogenation of acetylene (Fig. 3);

(3) the Rh(I) concentrations in Figs. 9 and 10 show maxima around the lower temperature maxima in the Rh 3*d*/Al 2*s* ratios; and

(4) the steep decreases in the Rh 3*d*/Al 2*s* and Cl/Rh ratios correspond to decreases in the Rh(I) fractions for both Rh-Y catalysts.

TABLE 4

Comparison between ESR Intensity of $g = 2.560$ Signal and Rh Metal Content Obtained with XPS for the Rh-Y(18%) Catalyst

Activation temperature (°C)	ESR intensity (arbitrary)	Rh metal content (% in Rh)
250	2.1	37
350	5.9	45
450	7.1	47

Accordingly, strong correlations are suggested among the activity, the chemical state, and the structure of Rh in the zeolites.

The superficial Si/Al atomic ratios were estimated from the Si 2*s*/Al 2*s* XPS area intensity ratios using the cross sections presented by Scofield (*19*). In the case of the Rh-Y (18%) zeolite, the calculated Si/Al ratio was 2.2, in good agreement with the nominal ratio (2.4). However, in the case of the Rh-Y (50%) zeolite, the Si/Al ratio was calculated to be 1.6, suggesting the partial decomposition of the zeolite structure. In our zeolite systems, no enrichment of SiO_2 was observed in the external surfaces of the zeolites, contrary to the observations by Tempere *et al.* (*20*).

DISCUSSION

Rh(I) as a stable intermediate oxidation state. It was found that Rh(I) was formed in the Rh-Y zeolite catalysts as a considerably stable intermediate during the reduction of Rh(III) to Rh metal by heat treatments in vacuum. The formations of

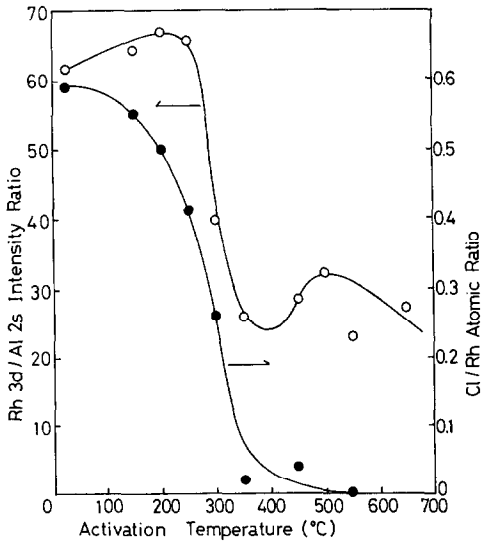

FIG. 11. Changes in the Rh 3*d*/Al 2*s* XPS intensity ratio and the Cl/Rh atomic ratio with activation temperature for the Rh-Y (50%) catalyst. ○, Rh 3*d*/Al 2*s*; and ●, Cl/Rh.

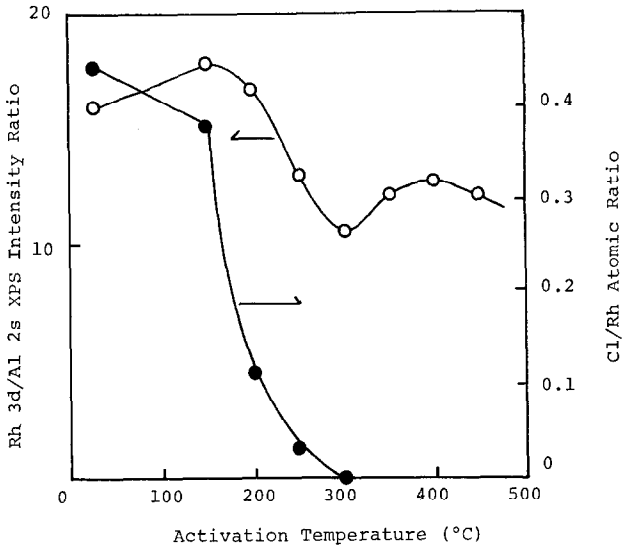

FIG. 12. Changes in the Rh 3*d*/Al 2*s* XPS intensity ratio and the Cl/Rh atomic ratio with activation temperature for the Rh-Y (18%) catalyst. ○, Rh 3*d*/Al 2*s*; and ●, Cl/Rh.

intermediate oxidation states of cations, Ni(I), Cu(I), and Pd(I), have been reported in the corresponding divalent transition metal cation-exchanged zeolites by reductions with CO, NO, and H_2 (*10–13*). However, the catalytic behavior of these intermediates has never been investigated. With regard to Rh(I) in the Rh-Y catalysts, the binding energy of the Rh $3d_{\frac{5}{2}}$ level (308.3 eV) falls between those for $RhCl(PPh_3)_3$ and $RhCl(CO)(PPh_3)_2$ or $RhH(CO)(PPh_3)_2$. These Rh complex catalysts show excellent activities for the hydrogenation of olefins (*14*). Therefore, Rh(I) in zeolite is expected, from the electronic state of Rh(I), to show high activities for reactions such as the hydrogenation of ethylene. Some residual chlorine may attach to Rh(I) to form Rh(I)Cl. The rest of the Rh(I) might exist as a bare Rh(I) cation and Rh(I)H, in which the hydride ion can be supposed to be the result of the decomposition of adsorbed H_2O (*21*). These Rh(I) cations are considered to be coordinatively unsaturated after the desorption of adsorbed H_2O, and hence they have high potentials to catalyze certain reactions.

Rh(I) is more stable in the Rh-Y (18%) zeolite than in the Rh-Y (50%). In the case of Rh-NH_4-Y (2.5% Rh), which were prepared by a cation exchange procedure using $RhCl_3 \cdot 3H_2O$ in excess ammonium solution, a considerable amount of Rh(I) continued to exist even after 700°C treatments (*22*). The lower the exchange degree of Rh, the more stable will be the intermediate oxidation state of Rh.

Rh(II) could not be detected in the Rh-Y zeolite catalysts with XPS and ESR. This is probably due to the instability of Rh(II) in zeolite framework. This agrees well with the fact that Rh(II) complexes can be formed only as special cases (*17, 18*).

Structure of Rh in zeolite. As shown in Figs. 11 and 12, the Rh 3*d*/Al 2*s* ratios changed considerably with activation temperature. The first slight increases are considered to result from the migration of Rh ion from the bulk on to the outermost surfaces of the zeolites, accompanied by the reduction of Rh(III) to Rh(I). Much more extensive segregations of cations in the zeolite outermost surfaces have been reported by Minachev *et al.* (*23*). Similar segregation phenomena have been ob-

served with XPS for supported MoO_3 and CoO catalysts (*24*, *25*).

Subsequent remarkable decreases in the Rh 3*d*/Al 2*s* ratios are considered to result from the formations of small Rh metal clusters, because no X-ray diffraction spectrum due to Rh metal could be obtained. The larger decrease in the Rh 3*d*/Al 2*s* ratios for the Rh-Y (50%) catalyst is due to the larger loading of Rh and, the greater extent of the reduction of Rh than in the Rh-Y (18%) catalyst. The clustering of Rh is considered to be strongly related to the reduction or decomposition of the Rh(I) cation. The following mechanisms can be proposed:

$$2\mathrm{Rh(I)Cl} \rightarrow 2\mathrm{Rh(0)} + \mathrm{Cl_2}$$
$$2\mathrm{Rh(I)H} \rightarrow 2\mathrm{Rh(0)} + \mathrm{H_2}$$
$$\mathrm{Rh(I)Cl} + \mathrm{Rh(I)H} \rightarrow 2\,\mathrm{Rh(0)} + \mathrm{HCl}$$
$$n\mathrm{Rh(0)} \rightarrow \mathrm{Rh}_n,$$

where Rh(0) denotes atomically dispersed Rh metal. The parallel decreases in the Rh(I) fraction, the Cl/Rh ratio, and the Rh 3*d*/Al 2*s* ratio are considered to substantiate the clustering mechanisms.

It is supposed that the subsequent small increases in the Rh 3*d*/Al 2*s* ratios, however, imply the migration of atomically dispersed Rh(0) and small clusters of Rh metal from the bulk to the outermost surface, accompanied by the subsequent formations of much larger Rh metal clusters and/or crystalline Rh metal, which may correspond to the second decreases in the Rh 3*d*/Al 2*s* ratios observed at higher activation temperatures [>400°C for the Rh-Y (18%) and >500°C for the Rh-Y (50%)]. As a matter of fact, in the case of the Rh-Y (50%) zeolite activated at 650°C, a very broad weak peak due to Rh metal was detected by X-ray diffraction techniques, and a slight loss in the crystallinity of the zeolite framework was observed too.

The Rh $3d_{\frac{5}{2}}$ binding energy for Rh metal will confirm the formation of Rh metal clusters and bulky crystalline Rh metal. When the Rh-Y (50%) catalyst was activated at 450°C, the binding energy of the Rh $3d_{\frac{5}{2}}$ level for Rh metal was 307.5 eV, which is higher by 0.3 eV than that for bulky Rh metal (307.2 eV), whereas it shifted to 307.2 eV when treated at 650°C. These findings are considered to reflect the particle size of Rh metal, taking into account the facts that an electron transfer from the metal to the zeolite can occur (*11*, *26*) and that the smaller the metal particle, the larger is the expected effect due to electron transfer (*27*).

Active state of Rh for the hydrogenation of ethylene. In the case of the Rh-Y (50%) zeolite catalyst, it is apparent that the LT maximum in the activity curve in Fig. 2 corresponds to the amount of Rh(I) in the zeolite in Fig. 9. It is immediately concluded that Rh(I) is active for the hydrogenation of ethylene. This is a very reasonable conclusion, since Rh(I) complex catalysts are well known to exhibit excellent activities for the hydrogenation of olefins (*14*). The reaction mechanisms are considered to be very similar to those in the homogeneous systems; that is, the oxidative addition of hydrogen to Rh(I), the insertion of hydride to adsorbed or coordinated ethylene, the formation of ethyl-σ-complex, and the subsequent reductive desorption of ethane.

The HT activity maximum in Fig. 2 corresponds to the HT maximum in Fig. 11, leading us to conclude that the hydrogenation of ethylene proceeds on Rh metal in this activation temperature region.

With the Rh-Y (18%) zeolite, completely identical conclusions can be drawn, comparing Figs. 2, 10, and 12.

Active state of Rh for the hydrogenation of acetylene. Comparing Figs. 3, 10, and 12, it is evident that the hydrogenation of acetylene proceeds on Rh metal but not on Rh(I). It is well known that bulky Rh metal is considerably active for the reaction (*28*). According to Wilkinson *et al.* (*29*),

TABLE 5

Effect of Pretreatment on the Rh Oxidation State in the Rh-Y(50%) Catalyst Activated at 250°C

Pretreatment gas	Pressure[a] (Torr)	Atomic fraction %		
		Rh (III)	Rh (I)	Rh metal
Nonpretreated		24	53	23
HCl[b]	13.8	38	46	16
	40.8	53	39	8
H_2[c]	24	15	61	24
H_2O[b]	0.5	40	52	8
	1.5	47	43	10

[a] The catalyst was pretreated with the indicated pressure of a gas for 30 min after the activation.

[b] Pretreated at room temperature.

[c] Pretreated at 50°C.

$RhCl(PPh_3)_3$, on the other hand, shows much less activity for the hydrogenation of alkynes than for the hydrogenation of alkenes. In addition, $RhH(CO)(PPh_3)_2$ does not show any activity for alkyne hydrogenation (*30*) probably due to too strong adsorption of the alkyne on the electron deficient Rh(I) complex. This is consistent with the fact that the Rh $3d_{\frac{5}{2}}$ binding energy for $RhH(CO)(PPh_3)_2$ is considerably higher than that for $RhCl(PPh_3)_3$ (Table 1). Therefore, it is very reasonable, taking into account the Rh $3d_{\frac{5}{2}}$ binding energy for Rh(I) in the zeolite catalysts, that Rh(I) shows no activity for the hydrogenation of acetylene and that the activity curve in Fig. 3 shows only a single peak responsible for metallic Rh.

Dimerization of ethylene on the Rh-Y catalysts. It is immediately concluded comparing Figs. 4, 9, 10, 11, and 12 that Rh(I) is the active state of Rh for the dimerization of ethylene, contrary to the conclusions by Yashima *et al.* (*9*). According to Cramer (*15*), Rh(I) complexes are active and the addition of HCl activates the catalysts in homogeneous systems. Similar phenomena are expected, provided that Rh(I) is an active species for the reaction in the zeolite systems. Actually, the pretreatment of the activated catalyst with HCl enhanced the activity of the catalyst for the dimerization of ethylene as shown in Fig. 6. The XPS studies of the pretreatment effects of the Rh-Y (50%) catalyst with HCl, H_2, and H_2O on the oxidation state of Rh cation are tabulated in Table 5. The admission of HCl caused decreases in the atomic fractions of Rh(I) and Rh metal, indicating the oxidative addition of HCl to Rh(0) and Rh(I) to form Rh(III) and Rh(I) hydride species. This is consistent with the case of $RhCl(PPh_3)_3$ exposed to HCl (Fig. 7). The following oxidative additions are proposed:

$$\mathrm{Rh(0)} + \mathrm{HCl} \rightarrow (\mathrm{Rh(II)HCl}) \rightarrow \tfrac{1}{2}\mathrm{Rh(I)H} + \tfrac{1}{2}\mathrm{Rh(III)HCl_2} \rightarrow \tfrac{1}{2}\mathrm{Rh(I)Cl} + \tfrac{1}{2}\mathrm{Rh(III)H_2Cl}$$

$$\mathrm{Rh(I)} + \mathrm{HCl} \rightarrow \mathrm{Rh(III)HCl},$$

and so on. The Rh(II) complex will disproportionate very easily to Rh(I) and Rh(III), since Rh(II) is unstable in the zeolite framework. The Rh species formed by the oxidative addition of HCl is active for the dimerization of ethylene, taking into account the mechanism proposed by Cramer (*15*). However, preadsorption of excess HCl will retard the reaction similar to CO, pyridine, and H_2O adsorbed on Rh or occluded in the zeolite cages by blocking chemically and/or physically the vacant coordination sites of Rh. Pretreatment of the catalyst with H_2 enhanced the catalytic activity for the reaction. This fact can be explained as follows: The amount of Rh(I) is increased by the reduction of Rh(III) (Table 5), and in addition, H_2 produces hydride species by oxidative addition which are active for the dimerization of ethylene.

CONCLUSIONS

Rh-Y zeolite catalysts were investigated with XPS. It is found that a con-

siderable amount of Rh(I) is produced as a stable intermediate during the reduction of Rh(III) to Rh metal by the heat treatment of the Rh-Y catalysts in vacuum. It is demonstrated that Rh(I) in the zeolites is active for the hydrogenation and the dimerization of ethylene and that Rh metal is active for the hydrogenation of both ethylene and acetylene. Strong correlations between homogeneous Rh complex systems and heterogeneous Rh-Y zeolite catalysts are found regarding the active state of Rh and probably the reaction mechanisms.

Rh in the zeolites shows considerable migration, clustering, and sintering during the activation process. It is suggested that the structure of Rh in the zeolite correlates strongly with the chemical nature of the Rh.

ACKNOWLEDGMENT

We are grateful to Prof. A. Nakamura (Osaka University) for giving us an opportunity to use a Du Pont 310 curve resolver.

REFERENCES

1. Van Sickle, D. E., and Prest, M. L., *J. Catal.* **19**, 209 (1970).
2. Mochida, I., Hayata, S., Kato, A., and Seiyama, T., *J. Catal.* **15**, 314 (1969); **19**, 405 (1970); **23**, 31 (1971).
3. Kubo, T., Kumada, F., Tominaga, H., and Kunugi, T., *Nippon Kagaku Kaishi*, 1621 (1972).
4. Pichart, P., Vedrine, J. C., Gallezot, P., and Imelik, B., *J. Catal.* **32**, 190 (1974).
5. Hatada, K., Ono, Y., and Keii, T., *Advan. Chem. Ser.* 501 (1973).
6. Coughlan, B., Narayanan, S., McCann, W. A., and Carroll, W. M., *J. Catal.* **49**, 97 (1977).
7. Chadle, G. D., Welsh, C. J., Dana, P. M., and Lappin, T. A., *Hydrocarbon Proc.* **45**, 103 (1966).
8. Rabo, J. A., Schomaker, V., and Pickert, P. E., *in* "Proceedings, 3rd International Congress on Catalysis, Amsterdam, 1964," Sect. 2, No. 4. Wiley, New York, 1965.
9. Yashima, T., Ushida, Y., Ebisawa, M., and Hara, N., *J. Catal.* **36**, 320 (1975).
10. Minachev, K. H., Antoshin, G. V., Shpiro, E. S., and Yusifov, Y. A., *in* "Proceedings, 6th International Congress on Catalysis, London, 1976" (G. C. Bonds and F. C. Thompkins, Eds.), Vol. 2, p. 621. Chemical Society, London, 1977.
11. Vedrine, J. C., Dufaux, M., Naccache, C., and Imelik, B., *J. Chem. Soc. Faraday Trans. I* **74**, 440 (1978).
12. Che, M., Dutel, J. F., Gallezot, P., and Primet, M., *J. Phys. Chem.* **80**, 2371 (1976).
13. Kasai, P. H., Bishop, R. J., Jr., and McLeod, D., Jr., *J. Phys. Chem.* **82**, 279 (1978).
14. Harmon, R. E., Gupta, S. K., and Brown, D. J., *Chem. Rev.* **73**, 21 (1973).
15. Cramer, R., *J. Amer. Chem. Soc.* **87**, 4717 (1965).
16. Wolsey, W. C., Reynold, C. A., and Kleinberg, J., *Inorg. Chem.* **2**, 463 (1963).
17. Cotton, F. A., and Wilkinson, G., "Advanced Inorganic Chemistry," 2nd Ed. Interscience, New York/London/Sydney, 1966.
18. Imanaka, T., Kaneda, K., Teranishi, S., and Terasawa, M., *in* "Proceedings, 6th International Congress on Catalysis, London, 1976" (G. C. Bonds and F. C. Thompkins, Eds.), Vol. 1, p. 509. Chemical Society, London, 1977.
19. Scofield, J. H., *J. Electron Spectrosc. Relat. Phenom.* **8**, 129 (1976).
20. Tempere, J. F., Delafosse, D., and Contour, J. P., *Chem. Phys. Lett.* **33**, 95 (1975).
21. Kasai, P. H., and Bishop, R. J., Jr., *J. Phys. Chem.* **81**, 1527 (1977).
22. Okamoto, Y., Ishida, N., Imanaka, T., and Teranishi, S., unpublished results.
23. Minachev, K. M., Antoshin, G. V., and Shpiro, E. S., *Izv. Akad. Nauk SSSR Ser. Khim.* **1015** (1974).
24. Okamoto, Y., Nakano, H., Shimokawa, T., Imanaka, T., and Teranishi, S., *J. Catal.* **50**, 447 (1977).
25. Okamoto, Y., Shimokawa, T., Imanaka, T., and Teranishi, S., *J. Catal.*, **50**, 153 (1979).
26. Escard, J., Pontivianne, B., and Contour, J. P., *J. Electron Spectrosc. Relat. Phenom.* **6**, 17 (1975).
27. Mason, M. G., and Baetzold, R. C., *J. Chem. Phys.* **64**, 27 (1976).
28. Bond, G. C., "Catalysis by Metals." Academic Press, London and New York, 1962.
29. Osborn, J. A., Jardin, F. H., Young, J. F., and Wilkinson, G., *J. Chem. Soc. A*, 1711 (1966).
30. O'Connor, C., and Wilkinson, G., *J. Chem. Soc. A*, 2665 (1968).